Clinical Investigative Study

Memory-Related Hippocampal Activity Can Be Measured Robustly Using fMRI at 7 Tesla

Nina Theysohn, MD, Shaozheng Qin, PhD, Stefan Maderwald, PhD, Benedikt A. Poser, PhD, Jens M. Theysohn, MD, Mark E. Ladd, PhD, David G. Norris, PhD, Elke R. Gizewski, MD, PhD, Guillen Fernandez, MD, PhD, Indira Tendolkar, MD, PhD

From the University Hospital Essen, Department of Diagnostic and Interventional Radiology and Neuroradiology, Essen, Germany (NT, SM, JMT, MEL) University Duisburg-Essen, Erwin L. Hahn Institute for Magnetic Resonance Imaging, Essen, Germany (NT, SM, BAP, JMT, MEL, DGN, ERG) Radboud University Nijmegen, Donders Institute for Brain, Cognition and Behaviour, Nijmegen, Netherlands (SQ, BAP, DGN, GF, IT) Stanford School of Medicine, Department of Psychiatry and Behavioral Science, Stanford, CA (SQ) University of Hawaii, Department of Medicine, Neuroscience and MR Research Program, Honolulu, HI (BAP) Department of Neuroradiology, University Hospital Innsbruck, Innsbruck, Austria (ERG) Radboud University Nijmegen Medical Centre, Department of Cognitive neuroscience, Nijmegen, Netherlands (GF, IT) Radboud University Nijmegen Medical Centre, Department of Cognitive neuroscience Psychiatry, Nijmegen, Netherlands (IT) University Hospital Essen, Department of Psychiatry and Psychotherapy, Essen, Germany (IT).

ABSTRACT

High field strength functional magnetic resonance imaging (fMRI) has developed rapidly. However, it suffers from increased artifacts in brain regions such as the medial temporal lobe (MTL), challenging functional imaging of the hippocampus with the objective of high-spatial resolution, which is particularly useful for this region both from a clinical and cognitive neuroscience perspective. We set out to compare a BOLD sequence at 7 T versus 3 T to visualize the MTL activity during an associative memory-encoding task. Twenty-eight healthy volunteers underwent a blocked-design fMRI at either 3 T or 7 T while performing a face-profession associative memory encoding task. Qualitative analyses of overall image quality revealed that functional images at 7 T were of high quality, showing a good white/gray matter contrast, with reasonably acceptable signal dropouts and artifacts at the lower portion of the temporal lobe. Analyses of task-related fMRI data revealed robust activations in the bilateral MTL during associative memory encoding at both field strengths. Notably, we observed significantly stronger memory-related hippocampal activation at 7 T than at 3 T, suggesting higher BOLD sensitivity at 7 T. These results are discussed in the light of the feasibility of 7 T scanning protocols for the MTL.

Keywords: Hippocampus, memory, ultra-high field strength MRI, fMRI, 7T.

Acceptance: Received July 11, 2012, and in revised form November 8, 2012. Accepted for publication February 23, 2013.

Correspondence: Address correspondence to Nina Theysohn, MD. E-mail: nina.theysohn@uk-essen.de.

Authors contributed equally.

J Neuroimaging 2013;23:445-451.
DOI: 10.1111/jon.12036

Introduction

In recent years high-resolution structural magnetic resonance imaging (MRI) has opened new possibilities to more optimally visualize small and complex anatomical regions in vivo, such as the medial temporal lobe (MTL) in particular the hippocampus.[1] This can be accomplished through an increase in field strength and consequently higher possible spatial resolution. Delineating the structural and functional integrity of hippocampal subregions and adjacent structures is an unmet need both for clinicians and cognitive neuroscientists, because it is vital to understanding the role of specific subregions given the core function of the MTL in the human declarative memory system.[2,3] However, functional investigation of memory-related functioning in the hippocampus is still mainly restricted to lower field strengths. In contrast with the well-established imaging of the hippocampus at 3 T and 1.5 T, little is currently known of functional imaging of the hippocampus involving an active memory task at ultra-high field such as 7 T.

Higher field strengths provide an increased image signal-to-noise ratio (SNR) and a supralinear increase of BOLD signal changes with the static magnetic field (B0);[4] both are important requirements for fast whole brain image acquisition with maximal sensitivity to BOLD signal changes.[5] Comparing 1.5, 3, and 7 T fMRI, van der Zwaag and colleagues recently showed in a simple motor task, that the calculated t-value as well as the percentage signal change in the motor cortex increased significantly with field strength.[6] These results suggest the feasibility of reliably detecting functional activity at high field strength.

Given the desire to routinely perform fMRI at high spatial resolution, there is great need to determine the optimal acquisition methodology and parameter settings for fMRI at (ultra-)high field[7] BOLD sensitivity is ultimately limited by the maximum available SNR, which is field strength dependent. In moving to smaller and smaller voxel sizes and higher acceleration factors, image SNR is eventually determined by thermal noise in the voxel and will scale linearly with the voxel volume.[8] In this high-resolution domain both the need for and potential benefits of high-field strengths are hence maximal. The supralinear increase in the BOLD signal change with field

strength[4] adds to this compelling motivation to optimize also high-resolution hippocampal fMRI at high field.

Most technical challenges in achieving this have been successfully addressed in the recent.[7] A couple of phenomena, however, are known to increase in severity with increasing field strength: The localization of the MTL close to the temporal and sphenoid bones, as for example the sphenoid sinus, leads to image distortions and signal drop-outs due to static magnetic field inhomogeneities in the anterior and medial parts of the hippocampus.[9] Some methodological refinements can overcome these problems. The impact of signal distortions can be reduced by decreasing the EPI readout time through accelerated parallel imaging with the help of multichannel coils.[10,11] Severe susceptibility-related signal dropouts at high field can be reduced by the use of optimized protocols, including optimization of the B0 shim, reduced slice thickness, optimized slice orientation to the inhomogeneity gradients, and the use of shorter echo times;[12] the latter however will result in reduced BOLD sensitivity in regions where the chosen echo time is much shorter than the T2* relaxation time of the local gray matter. Thus, it is feasible to measure functional activity of the hippocampus at 7 T by using accelerated parallel imaging with optimized protocols. With respect to the hippocampus, improvement of paradigms and longer scan durations can improve the depiction of functional hippocampal activity at clinical field strengths.[13] Furthermore, studies using optimized slice-tilt, phase encoding direction and z-shim moment[14] suggest that this may be in particular useful for higher field strength opening up possibilities to optimize MTL scanning at 7 T. The second expected improvement in signal quality that may be relevant for imaging the MTL at high-field strength can be achieved by technical improvements of hardware components, especially by multichannel coils. For example Bellgowan and colleagues showed an increased contrast to noise ratio (CNR) and an improvement of SNR by using a 16-element surface coil array at 3 T simultaneously with smaller voxel sizes.[15] In the light of the aforementioned findings, one may conjecture that optimized functional imaging of the MTL at 7 T would be feasible to measure functional activity of the hippocampus, and would also increase sensitivity to detecting nuanced hippocampal activity during an active memory task, thereby providing new options for high resolution scanning of this brain region.

To test this hypothesis, we set up a study using fMRI at 3 and 7 T to examine memory-related hippocampal activity during an associative memory task. At 7 T we utilized a custom built multichannel head coil allowing for parallel imaging and voxel size reduction[16] and a 2-D EPI sequence with an improved shim algorithm to optimize functional imaging of the MTL by reducing signal drop-outs and distortion. Meanwhile, a blocked design with associative memory-encoding task was used in which a slow BOLD response can be made more compatible with slow on and off variation and a potential misspecification of the hemodynamic response function will not impact on the fit of the model. We used such a blocked design because it may also be in particular relevant for future clinical studies.[17] We expected that functional imaging of the MTL at 7 T would yield similar pattern of memory-related activations in the MTL as observed at 3 T by using a standard sequence in our previous studies.[18,19] Furthermore we expected that functional imaging at 7 T would boost the sensitivity to BOLD changes in the hippocampus compared to 3 T.

Materials and Methods

Subjects

Twenty-eight young healthy, right-handed volunteers (12 males, mean age ± SD 26.1 ± 2.8 years; range 20-38 years) were examined. All subjects reported no history of neurological or psychiatric disease, and did not have any current medication. The study was approved by the local ethics committee. All participants gave written informed consent prior to participation. Participants were randomly assigned to either being scanned at a 7 T or at a 3 T MRI-scanner. There was no significant difference between both scanning groups with respect to age, gender, and level of education.

Stimuli

Stimuli consisted of 16 portraits (half males) and 16 familiar professional names which were randomly paired for each subject. Stimuli were standardized along several criteria such as direct gaze contact, no strong emotional facial expression, no headdress, no glasses, no beard, etc.[20] Length of familiar professional names ranged from 3-10 letters (mean length ± SD = 4.6 ± 1.5).

Associative Memory Encoding Task and Subsequent Memory Test

Using a blocked-design, subjects underwent four blocks of an active condition (ie, associative memory encoding task) interleaved by five blocks of a control condition; each block lasted 30 seconds. In total, the task session lasted 4.5 minutes. For the associative memory condition, each block started with the presentation of a brief instruction for 2 seconds, then followed by showing a series of four novel faces uniquely associated with professional names. Each face with its associated professional name underneath was displayed at the center of screen for 5.7 seconds. Subjects were instructed to memorize face-profession association for a subsequent memory test and to make a judgment whether the face fitted well the underlined profession or not. A simple visuo-motor task was used as control condition, in which each block started with the presentation of a brief instruction for 2.0 seconds, and followed by showing a series of six shadow-masked face contours with the presentation time of 3.8 seconds each. Subjects were asked to judge whether the ear of a shadow-masked face contour was nearer to the left or the right shoulder. Around 10 minutes later, subjects performed two associative memory tests outside the scanner. In the first memory test, each studied face was presented as a cue, and subjects had to recall the associated profession of this person at the study phase. In the second test subjects had to select the recalled professions out of a written list consisting of all presented professions.

Data Acquisition

Prior to sequence acquisition, shimming at 3 T (Siemens Trio 3 T, Erlangen, Germany) was performed automatically with

the standard shimming algorithm available on the scanner. Scanning at 7 T (Siemens Magnetom 7 T, Erlangen, Germany) required manual shimming by the user, including the standard Siemens shimming algorithms in conjunction with multiple repeats of the B_0 shimming tool which was provided by the vendor (Work in Progress, WIP 450B). It is a gradient echo sequence whose reconstruction algorithm is based on the work of Schar et al.[21] These results were used for frequency adjustment. For B_1 field mapping, eg, transmitter adjustments, an additional vendor-provided spin-echo type sequence (WIP 397) was used. After a slice selective excitation, two refocusing pulses generate a spin-echo and a stimulated echo, respectively. The algorithm is mainly based on the work of Hoult.[22] Finally, the shim results were carefully verified before starting the T2*-weighted gradient echo EPI sequence. The phase correction parameters for Nyquist ghost correction were calculated shot by shot using three non-phase-encoded navigator echoes before the EPI readout,[23] which also moreover allowed the effects of scanner frequency drift to be removed during image reconstruction. For imaging data at 3 T, whole brain T2*-weighted EPI-BOLD fMRI data were acquired with a 32 channel head coil (both Siemens Healthcare, Erlangen, Germany) using an ascending slice acquisition sequence and no GRAPPA (37 paraaxial slices, volume TR 2,180 milliseconds, TE 25 milliseconds, flip angle 80°, matrix size 64*64, slice thickness 3.0 mm, slice gap 0.3 mm, field of view 212*212 mm^2) bandwidth 1,906 Hz/pixel, echo spacing 0.59 milliseconds.[18] Structural images (1*1*1 mm^3) were acquired using a T1-weighted 3D MP-RAGE sequence (TR 2,300 milliseconds, TE 2.96 milliseconds, flip-angle 8°, 192 contiguous sagittal slices, matrix size 256*256, FOV 256*256 mm^2). Image acquisition at 7 T was performed on a whole-body MR system with an 8-channel, custom built, meander transmit/receive head coil.[24] Whole brain gradient echo EPI images were acquired using an ascending slice acquisition order and Siemens' integrated parallel acquisition technique (iPAT) in conjunction with a GRAPPA acceleration factor of t2 (46 reference lines per slice acquired at start of the scan). The imaging parameters were 50 paraaxial slices of 2.0 mm, no slice GAP, TR 2,050 milliseconds, TE 25 milliseconds, flip angle 70°, matrix size 92 * 92, FOV 230 * 230 mm^2, in-plane resolution 2.5*2.5 mm^2, bandwidth 2,090 Hz/pixel, echo spacing 0.56 milliseconds. These parameters were chosen after careful optimization of the protocol with respect to overall image quality, temporal stability, reduction of Nyquist ghosting, quality of the parallel imaging reconstruction and artifact levels especially in the region surrounding the MTL. Taking into account the field strength dependence and imaging parameters, image distortion at 7 T was expected to be only marginally (factor 1.1) higher than at 3T. Structural images at 1 mm isotropic resolution were again acquired using an MP-RAGE sequence (TR 3,000 milliseconds, TE 2.19 milliseconds, TI 1,100 milliseconds, flip angle 7°, 256 contiguous sagittal slices, matrix size 256*256, FOV 256*256 mm^2).

Data Analysis

Image preprocessing and statistical analysis were performed using SPM5 (Welcome Department of Cognitive Neurology, London, UK). The first five EPI volumes were discarded to allow for T1 equilibration. Remaining functional images were rigid-body motion corrected. Distortion correction was not applied; however this does not compromise comparability of the two datasets since they were approximately equally affected by distortion for the EPI protocols used in this study. Images were then transformed into the MNI space (averaged EPI template for the 3 and 7 T data) and resampled into 2 mm isotropic voxels. Finally, images were spatially smoothed by convolving with a 6 mm isotropic 3D-Gaussian kernel. The data were statistically analyzed using general linear models (GLM) and statistical parametric mapping. To assess neural activity related to associative memory encoding, the active condition was modeled as a box-car regressor and convolved with the canonical hemodynamic response function in SPM5.[25] High-pass filtering with a cut-off of 128 seconds were applied and serial correlations correction using a first-order autoregressive (or AR [1]) model. The contrast parameter images for the active condition relative to the control condition (or baseline), which were generated at the single-subject level, were submitted to a second-level analysis conducting a two-sample independent t-test (3 T vs. 7 T) while treating subjects as random effect. A whole brain analysis was performed, initially thresholded at $P < .001$ (uncorrected), whereby cluster size statistics were used subsequently as the test statistic. Unless otherwise specified, only clusters significant at $P < .05$ corrected for multiple comparisons will be reported. To examine the regional overlap between two datasets, an additional conjunction analysis was performed using the minimum statistic compared with the conjunction null method as implemented within SPM5.[26] To further characterize patterns of hippocampal activation related to associative memory encoding at the two field strengths, we conducted region of interest (ROI) analyses on extracted and averaged data for the bilateral anatomically defined hippocampus ROIs.[27,28] Beta values were extracted from these ROIs by using MarsBar, and then submitted to further statistical tests in SPSS (16.0, SPSS Inc, Chicago, USA).

Results

Behavioral Results

Subjects in the 3 T group showed a mean cued recall of 47.8% (± 4.6%) while subjects in the 7 T group recalled 52.3% (± 9.6%). The performance of the cued-recall test in the two groups is highly significantly above chance level of zero at both 3 T and 7 T (both $t(23) > 5.20$, $P < .001$), indicating successful memory formation. Importantly, there was no significant difference ($t < 1$) between subjects participating in either the 3 T or the 7 T group, indicating that differences in memory performance cannot account for differences observed at the neural imaging level.

Hippocampal Activations in Associative Memory Encoding at 3 T and 7 T

Figure 1 shows two typical EPI-images acquired at 3 T (Fig 1A) and 7 T (Fig 1B). An overview of all whole brain activities, related to associative memory encoding is given in Table 1. To assess neural activity related to associative memory encoding, we contrasted the active condition (ie, associative encoding

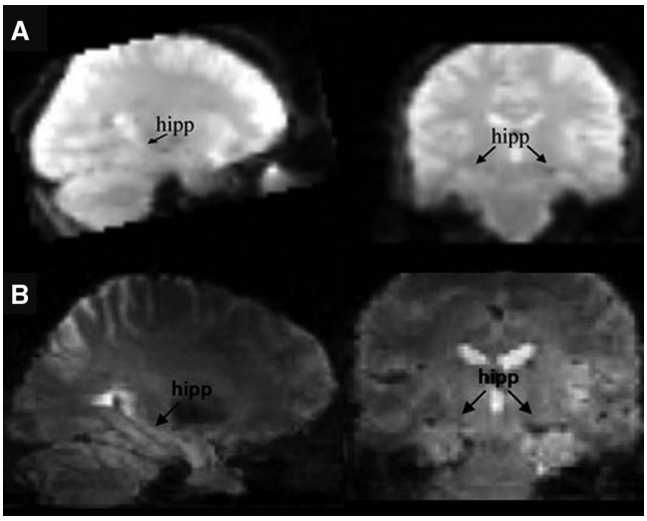

Fig 1. Single subject analysis: selection of acquired EPI images in representative slices along the hippocampus at (A) 3 T and (B) 7 T. A resolution of 3*3*3 mm^3 with 37 axial slices at 3 T and 2.5*2.5*2 mm^3 with 50 axial slices at 7 T leads to whole brain coverage. The hippocampus is marked with arrows bilateral in coronar slices and unilateral in sagittal slices. Although suffering from minor distortions and signal dropouts temporobasal at 7 T the anatomical correlate of the hippocampal and parahippoampal structures can be identified in coronar slices and are well defined in the sagittal slice.

Table 1. Brain Activations Related to Associative Memory Encoding

Brain Regions	R/L	BA	T Values	Cluster Size	Coordinates MNI
Active condition versus control condition at 3 T					
Posterior visual cortex	R	18	8,17	4,849***	20 −102 −8
	L		5.52		−24 −82 −20
Hippocampus	R	–	6.81	2,062***	30 −22 −14
	L	–	8.13		−26 −18 −16
PHC	L	30	7.14		−12 −30 −6
Inferior PFC	L	47	7.27	482***	−42 24 −16
Medial PFC	L	10	5.92	442***	0 62 14
	L	11	7.02	185 ***	−4 40 −16
Active condition versus control condition at 7 T					
Posterior visual cortex	R	18	10.26	2,540***	20 −98 12
	L		13.29		−16 −102 2
Hippocampus	R	35	7.22	313***	22 −24 −18
	L		10.18	1,789***	−24 −26 −16

***$P < .05$ whole brain cluster level corrected. PFC, prefrontal cortex; PHC, parahippocampal cortex; L, left; R, right; BA, Brodmann Area; MNI, Montreal Neurological Institute in SPM5.

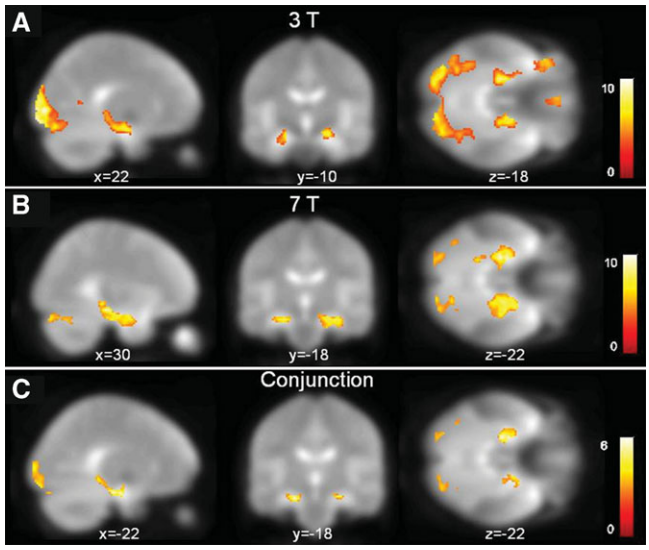

Fig 2. (A, B) Statistical parametric maps of activation within all subjects performing the associative memory task compared with the control condition at 3 T (A) and 7 T (B) in a one sample t-test thresholded at $P < .05$. Representative sagittal, coronal, and axial slices show bilateral activation of the hippocampus and the posterior visual cortex at both field strengths. (C) Statistical parametric maps of a conjunction analysis show clear spatial overlap between the two datasets (3 T and 7 T) in the bilateral hippocampus.

Table 2. A: Overlap in Brain Activation Related to Associative Memory Encoding at 3 T and 7 T. B: Two –Sample t-Test between 3 T and 7T Showing the Contrast 7T > 3T

Brain Regions	R/L	BA	T Values	Cluster Size	Coordinates MNI
A: Conjunction (Active vs. control) at 3 T and 7 T					
Posterior visual cortex	R	18	7.28	841***	14 −102 10
	L	18	7.13		−16 −104 6
Hippocampus	R	HC	5.90	203***	30 −24 −16
	L	35	6.30	375***	−22 −14 −22
Inferior PFC	L	47	7.27	482***	−36 28 −20
B: 7 T > 3 T					
Hippocampus	R	HC	6.08	632***	34 −18 −20
	L	35	5.56	201***	−28 −26 −18
PCC	–	31	5.35	402***	0 −60 26
Posterior visual cortex	R	18	5.72	305***	−12 −102 −8
	L	18	5.24	257***	10 −100 12

***$P < .05$ whole brain cluster level corrected. PFC, prefrontal cortex; PCC, posterior cingulated cortex; L, left; R, right; BA, Brodmann Area; MNI, Montreal Neurological Institute in SPM5.

of face-profession names) with the control condition in both datasets separately. For the dataset at 3 T, results revealed robust functional activations in the bilateral MTL especially for the hippocampus, the left inferior prefrontal cortex, the ventral medial prefrontal cortex, and the posterior visual cortex (Fig 2A; Table 1). For the dataset at 7 T, we also found very robust activations in the bilateral MTL including in the hippocampus as well as the posterior visual cortex (Fig 2B; Table 1). To ensure actual overlap of activation patterns between the two datasets, we conducted a conjunction analysis over the two contrasts, indicating that the bilateral hippocampus indeed exhibited strong activations during associative memory encoding (Fig 2C; Table 2).

More importantly, we directly compared functional activity related to associative memory encoding at 7 T with 3 T. This contrast revealed significantly higher activation in the hippocampus bilaterally as measured with 7 T (Fig 3A; Table 2). To better characterize the intensity of the hippocampal activation, we performed a region of interest analysis for the bilateral hippocampus anatomically defined. Beta values or parameter estimates (in arbitrary units) were extracted for the active versus control condition for each subject. A two-independent

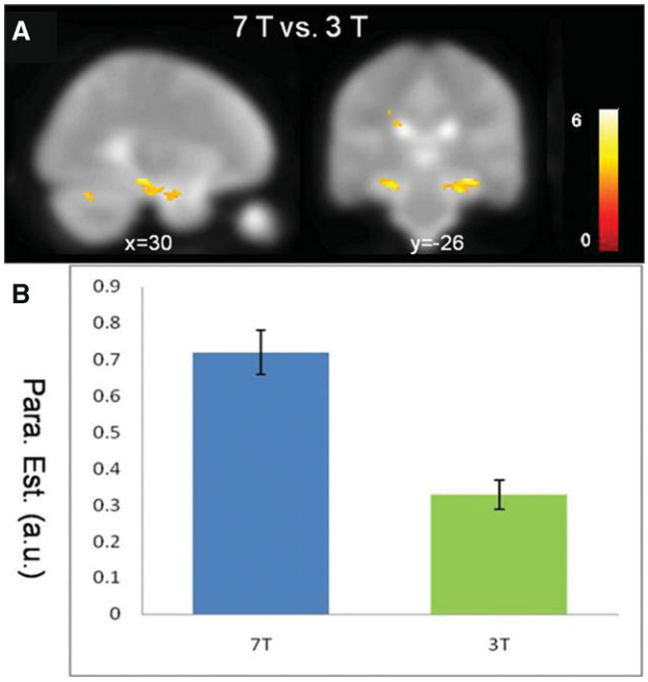

Fig 3. (A) Field strength comparison: a two sample t-test (contrast 7 T vs. 3 T) shows a plus in BOLD sensitivity in bilateral hippocampus at 7 T. (B) Box plot comparison of 3 T (right) and 7 T (left) datasets. Extracted beta values of parameter estimation show significant higher intensity of the hippocampal activation at 7 T (0.7 ± 0.06 at 7 T vs. 0.33 ± 0.04 at 3 T).

samples t-test revealed significantly stronger hippocampal activation at 7 T (0.72 ± 0.06) than 3 T (0.33 ± 0.04) ($t(23) = 5.63$; $P < .001$) (Fig 3B). Together these results indicate a parallel pattern of functional activation related to associative memory encoding at both field strengths, particularly with higher levels of hippocampal activation at 7 T than at 3 T.

Discussion

In this feasibility study we compared functional activity of the hippocampus involved in associative memory encoding as measured at 3 T and 7 T by using an optimized sequence. As expected, we were able to replicate robust functional activation related to associative memory encoding within the MTL at 3 T and 7 T, indicating the feasibility of our EPI sequence at high field strength. Notably, we found significantly higher levels of hippocampal activations at 7 T than at 3 T, suggesting higher sensitivity to detect memory-related hippocampal activity at high field strength. Below, we will discuss our observed increase in hippocampal activation at 7 T within the framework of higher sensitivity to BOLD signal changes at high field strength.

Our data are in line with previous findings showing significantly higher sensitivity to detect functional activation of the primary motor cortex at a 7 T system compared to either 1.5 T or 3 T, as measured by percent signal change, mean t-values, number of suprathreshold voxels and contrast to noise ratio.[29,30] When directly comparing functional activity in high resolution EPI images at 3 T versus 7 T, for instance, Hoffmann and colleagues found that 3 T images were more seriously affected by noise compared to 7 T thereby reducing BOLD sensitivity.[31] Hale and colleagues compared functional connectivity measurements at 7 T with 3 T, and they also found that BOLD contrast to noise ratio increases with magnetic field strength.[32] The authors found that spatial correlations, dependent on the SNR, increased at 7 T compared to 3 T. Here we extend these previous findings by providing initial evidence that our EPI sequence at 7 T are able to outperform 3 T in terms of quantitative sensitivity to functional activation within the MTL. More specifically our results are also consistent with a recent study by Sladky et al reporting significantly higher BOLD signal changes at 7 T in the amygdala,[33] a region also being critical for functional imaging at higher field strength due to its temporobasal localization near the sphenoid sinus. Our observed higher functional activity at 7 T may result from an improvement in SNR at higher field strength. Indeed it has been shown that the BOLD contrast to noise ratio can improve with increasing field strength.[4] Several important features implemented in our study support this notion. First, we had to use high spatial resolution as the BOLD noise, being also T2*-dependent, was found to rise with increasing field strength.[34] This confound can be reduced by using higher spatial resolution during image acquisition at high field strength.[8] Second, as recommended in the literature, EPI image quality can be optimized by a shim algorithm using a 3-D head shim prior to sequence acquisition in order to reduce B0 magnetic field inhomogeneities.[35] Slice-wise B0 shimming is in principle attractive and may optimize the shim for multiple regions across the brain and hence reduce distortions and through-plane signal losses;[36] however it has not as yet proven itself in routine application, largely because it requires additional time and lengthens the repetition time. It is also not readily compatible with standard sequences on clinical MRI systems. In our set up at 7 T we used parallel imaging and a custom build multi channel head coil to further improve image quality in the MTL by increasing resolution to 2.5 mm in plane and 2 mm through plane. Previously investigated at 3 T and recently proved at 7 T, multiecho EPI sequences have been shown to reduce image artifacts and acquire images at multiple TEs following a single excitation.[37–39] Moreover, three dimensional isotropic EPI sequences (3D-EPI) may also offer a promising alternative to 2D EPI for high field fMRI, as it has been shown to allow improved SNR and lower levels of artifacts, and, in conjunction with appropriate receive coil arrays allows considerable TR reduction by acceleration along the slice direction.[40–42] Especially at 7 T, 3D-EPI techniques open new possibilities for event related functional MRI since further investigation of higher cognitive functions such as the memory system is challenging with blocked designs. Hence, we believe that the impact of signal dropouts in the MTL could be reduced[12,43–45] in the present study, for instance by further optimizing slice orientation and reducing slice thickness. In our case the echo time could not be further reduced without compromising in-plane resolution or forcing the choice of a higher GRAPPA acceleration factor, which during initial test scans was found to result in much reduced image quality. With respect to the applied spatial smoothing (6 mm FWHM) we went for a tradeoff between the highest possible SNR without relevant

reduction of spatial resolution,[46] since we have expected a higher intrinsic SNR at 7T. Further efforts to optimize the sequence toward specific regions in the medial temporal or prefrontal cortex may include the use of slice-dependent echo time,[47] slice dependent slice thickness, or the application of z-shim moment to counter through-plane dephasing.[14,48,49] A few limitations have to be taken into account. Firstly, identical parameters concerning at least in- and through-plane resolution in 3 T and 7 T may have improved the direct comparison of MTL activation at both field strengths. But for our question at issue the sequence was optimized for whole brain coverage at 7 T and compared to an established 3 T sequence. While very high quality images could be acquired on the vast majority of subjects, on the other hand, three out of 14 subjects of 7 T datasets suffered from considerably increased artifacts. These in particular included temporally unstable Nyquist ghosting, which varied between subjects despite the same protocols being used, and appeared to be related to the quality of the shim.[50] Both concerns can however be addressed using a promising recent improvement in single-shot EPI acquisition, which at 7T has been demonstrated to yield essentially ghost-free images, and hence much improved temporal stability thanks to the absence of fluctuating Nyquist ghosts.[51] Finally, signal distortions did lead to minor displacements of hippocampal activity compared to 3 T as the local cluster maximum differed between the two groups (as shown in Table 2), however conjunction analysis of 3 T and 7 T revealed a strong overlap of functional activity in the hippocampus indicating the relative displacement was small (factor 1.1). Individual differences between the 3 T and 7 T subject pools may also have contributed since the set-up of the study unfortunately did not allow us to scan the same subjects on both scanners. One possibility to address these issues is the use of EPI distortion correction[52,53] which improves the registration between individual subjects' structural and functional data, and has also been shown to improve activation detection at the group level.[54] In this study the scan protocol was carefully set up within the technical challenges and limitations posed by high field fMRI. While these limitations were apparent in some subjects, the results revealed a robust BOLD response in the bilateral hippocampus related to associative memory encoding at 7 T. Hence the present results show that functional MRI of the MTL is feasible at 7 T even with a whole brain sequence. The higher BOLD signal sensitivity at 7 T compared to 3 T may additionally indicate that using well-chosen protocols and hardware may even give an advantage to functional imaging of the MTL in the future. Future high-field fMRI studies imaging the MTL should focus on high resolution sequences (1 or 1.5 mm^3) because smaller voxel volumes have resulted in reduced partial volume effects, more detailed spatial resolution and allow for an improved function to anatomy correspondence.[31,55] To achieve further improvements in resolution, artifact reduction and acceleration, coil improvements (16 channel and higher) are needed.[56] Especially for the MTL, where the anterior and medial part is supposed to be a critical region concerning functional results to cognitive tasks higher coil dimensionality should lead to a significant SNR improvement that permits further reduction of slice thickness.[15] In conjunction with volumetric sequences (eg, 3D-EPI) they moreover allow drastic TR reductions as they permit parallel acceleration along the secondary phase encoding direction.

Conclusion

In conclusion, our data provide initial evidence that a rather standardized scan setting at 7 T allows good visualization of memory-related MTL function. In the light of the gain in SNR at higher field strength the results from our comparison between 3 T and 7 T further suggest that optimized MTL scanning at 7 T is not only feasible with short paradigms but may even show higher sensitivity to detecting subtle changes in the BOLD signal, which may be in particular relevant in the improvement of functional MTL imaging in health as well as in diseases.

References

1. Theysohn JM, Kraff O, Maderwald S, et al. The human hippocampus at 7 T–in vivo MRI. *Hippocampus* 2009;19:1-7.
2. Eichenbaum H, Yonelinas AP, Ranganath C. The medial temporal lobe and recognition memory. *Annu Rev Neurosci* 2007;30:123-152.
3. Squire LR, Stark CE, Clark RE. The medial temporal lobe. *Annu Rev Neurosci* 2004;27:279-306.
4. Yacoub E, Shmuel A, Pfeuffer J, et al. Imaging brain function in humans at 7 Tesla. *Magn Reson Med* 2001;45:588-594.
5. Balteau E, Hutton C, Weiskopf N. Improved shimming for fMRI specifically optimizing the local BOLD sensitivity. *Neuroimage* 2010;49:327-336.
6. van der Zwaag W, Francis S, Head K, et al. fMRI at 1.5, 3 and 7 T: characterising BOLD signal changes. *NeuroImage* 2009;47:1425-1434.
7. Barth M, Poser, B.A. Advances in high-field BOLD fMRI. *Materials* 2011;4:1941-1955.
8. Triantafyllou C, Polimeni JR, Wald LL. Physiological noise and signal-to-noise ratio in fMRI with multi-channel array coils. *NeuroImage* 2011;55:597-606.
9. Krasnow B, Tamm L, Greicius MD, et al. Comparison of fMRI activation at 3 and 1.5 T during perceptual, cognitive, and affective processing. *NeuroImage* 2003;18:813-826.
10. de Zwart JA, Ledden PJ, van Gelderen P, et al. Signal-to-noise ratio and parallel imaging performance of a 16-channel receive-only brain coil array at 3.0 Tesla. *Magn Reson Med* 2004;51:22-26.
11. Preibisch C, Wallenhorst T, Heidemann R, et al. Comparison of parallel acquisition techniques generalized autocalibrating partially parallel acquisitions (GRAPPA) and modified sensitivity encoding (mSENSE) in functional MRI (fMRI) at 3T. *J Magn Reson Imaging* 2008;27:590-598.
12. Speck O, Stadler J, Zaitsev M. High resolution single-shot EPI at 7T. *Magma* 2008;21:73-86.
13. Bakker A, Kirwan CB, Miller M, et al. Pattern separation in the human hippocampal CA3 and dentate gyrus. *Science* 2008;319:1640-1642.
14. Weiskopf N, Hutton C, Josephs O, et al. Optimal EPI parameters for reduction of susceptibility-induced BOLD sensitivity losses: a whole-brain analysis at 3 T and 1.5 T. *NeuroImage* 2006;33:493-504.
15. Bellgowan PS, Bandettini PA, van Gelderen P, et al. Improved BOLD detection in the medial temporal region using parallel imaging and voxel volume reduction. *NeuroImage* 2006;29:1244-1251.
16. Thurling M, Kuper M, Stefanescu R, et al. Activation of the dentate nucleus in a verb generation task: a 7T MRI study. *NeuroImage* 2011;57:1184-1191.
17. Putcha D, O'Keefe K, LaViolette P, et al. Reliability of functional magnetic resonance imaging associative encoding memory paradigms in non-demented elderly adults. *Hum Brain Mapp* 2011;32:2027-2044.

18. Qin S, van Marle HJ, Hermans EJ, et al. Subjective sense of memory strength and the objective amount of information accurately remembered are related to distinct neural correlates at encoding. *J Neurosci* 2011;31:8920-8927.
19. Qin S, Hermans EJ, van Marle HJ, et al. Understanding low reliability of memories for neutral information encoded under stress: alterations in memory-related activation in the hippocampus and midbrain. *J Neurosci* 2012;32:4032-4041.
20. Qin S, Piekema C, Petersson KM, et al. Probing the transformation of discontinuous associations into episodic memory: an event-related fMRI study. *NeuroImage* 2007;38:212-222.
21. Schar M, Kozerke S, Fischer SE, et al. Cardiac SSFP imaging at 3 Tesla. *Magn Reson Med* 2004;51:799-806.
22. Hoult DI. The Principle of Reciprocity. *J Magn Reson.* 2011;213(2):344-346.
23. Heid O. *Robust EPI Phase Correction.* Vancouver: ISMRM, 1997:p. 2014.
24. Orzada S, Kraff O, Schäfer LC, et al. 8-Channel Transmit/receive Head Coil for 7 T Human Imaging Using Intrinsically Decoupled Strip Line Elements with Meanders. *17th Annual Meeting of ISMRM* Honolulu, Hawaii, USA; 2009.
25. Friston KJ, Mechelli A, Turner R, et al. Nonlinear responses in fMRI: the Balloon model, Volterra kernels, and other hemodynamics. *Neuroimage* 2000;12:466-477.
26. Nichols T, Brett M, Andersson J, et al. Valid conjunction inference with the minimum statistic. *NeuroImage* 2005;25:653-660.
27. Tzourio-Mazoyer N, Landeau B, Papathanassiou D, et al. Automated anatomical labeling of activations in SPM using a macroscopic anatomical parcellation of the MNI MRI single-subject brain. *NeuroImage* 2002;15:273-289.
28. Qin S, Rijpkema M, Tendolkar I, et al. Dissecting medial temporal lobe contributions to item and associative memory formation. *NeuroImage* 2009;46:874-881.
29. Beisteiner R, Robinson S, Wurnig M, et al. Clinical fMRI: evidence for a 7T benefit over 3T. *NeuroImage* 2011;57:1015-1021.
30. Gizewski ER, de Greiff A, Maderwald S, et al. fMRI at 7 T: whole-brain coverage and signal advantages even infratentorially? *NeuroImage* 2007;37:761-768.
31. Hoffmann MB, Stadler J, Kanowski M, et al. Retinotopic mapping of the human visual cortex at a magnetic field strength of 7T. *Clin Neurophysiol* 2009;120:108-116.
32. Hale JR, Brookes MJ, Hall EL, et al. Comparison of functional connectivity in default mode and sensorimotor networks at 3 and 7T. *Magma* 2010;23:339-349.
33. Sladky R, Baldinger P, Kranz GS, Trostl J, Hoflich A, Lanzenberger R, et al. High-resolution functional MRI of the human amygdala at 7T. *Eur J Radiol* 2011;82(5):728-733.
34. Kruger G, Glover GH. Physiological noise in oxygenation-sensitive magnetic resonance imaging. *Magn Reson Med* 2001;46:631-637.
35. Carr VA, Rissman J, Wagner AD. Imaging the human medial temporal lobe with high-resolution fMRI. *Neuron* 2010;65:298-308.
36. Sengupta S, Welch EB, Zhao Y, et al. Dynamic B0 shimming at 7 T. *Magn Reson Imaging* 2011;29:483-496.
37. Poser BA, Norris DG. Investigating the benefits of multi-echo EPI for fMRI at 7 T. *NeuroImage* 2009;45:1162-1172.
38. Poser BA, Versluis MJ, Hoogduin JM, et al. BOLD contrast sensitivity enhancement and artifact reduction with multiecho EPI: parallel-acquired inhomogeneity-desensitized fMRI. *Magn Reson Med* 2006;55:1227-1235.
39. Schmiedeskamp H, Newbould RD, Pisani LJ, et al. Improvements in parallel imaging accelerated functional MRI using multiecho echo-planar imaging. *Magn Reson Med* 2010;63:959-969.
40. Poser BA, Koopmans PJ, Witzel T, et al. Three dimensional echo-planar imaging at 7 Tesla. *NeuroImage* 2010;51:261-266.
41. van der Zwaag W, Marques JP, Kober T, Glover G, Gruetter R, Krueger G. Temporal SNR characteristics in segmented 3D-EPI at 7T. *Magn Reson Med* 2011;67(2):344-352.
42. Zwanenburg JJ, Versluis MJ, Luijten PR, et al. Fast high resolution whole brain T2* weighted imaging using echo planar imaging at 7T. *NeuroImage* 2011;56:1902-1907.
43. Chen NK, Dickey CC, Yoo SS, et al. Selection of voxel size and slice orientation for fMRI in the presence of susceptibility field gradients: application to imaging of the amygdala. *NeuroImage* 2003;19:817-825.
44. Merboldt KD, Finsterbusch J, Frahm J. Reducing inhomogeneity artifacts in functional MRI of human brain activation-thin sections vs gradient compensation. *J Magn Reson* 2000;145:184-191.
45. Olman CA, Davachi L, Inati S. Distortion and signal loss in medial temporal lobe. *PLoS One* 2009;4:e8160.
46. Mikl M, Marecek R, Hlustik P, et al. Effects of spatial smoothing on fMRI group inferences. *Magn Reson Imaging* 2008;26:490-503.
47. Stocker T, Kellermann T, Schneider F, Habel U, et al. Dependence of amygdala activation on echo time: results from olfactory fMRI experiments. *NeuroImage* 2006;30:151-159.
48. Deichmann R, Gottfried JA, Hutton C, et al. Optimized EPI for fMRI studies of the orbitofrontal cortex. *NeuroImage* 2003;19:430-441.
49. Gottfried JA, Deichmann R, Winston JS, et al. Functional heterogeneity in human olfactory cortex: an event-related functional magnetic resonance imaging study. *J Neurosci* 2002;22:10819-10828.
50. van der Zwaag W, Marques JP, Lei H, et al. Minimization of Nyquist ghosting for echo-planar imaging at ultra-high fields based on a "negative readout gradient" strategy. *J Magn Reson Imaging* 2009;30:1171-1178.
51. Poser BA, Barth M, Goa PE, Deng W, Stenger VA. Single-shot echo-planar imaging with Nyquist ghost compensation: Interleaved dual echo with acceleration (IDEA) echo-planar imaging (EPI). *Magn Reson Med* 2012;69(1):37-47.
52. Hutton C, Bork A, Josephs O, et al. Image distortion correction in fMRI: a quantitative evaluation. *NeuroImage* 2002;16:217-240.
53. Zaitsev M, Hennig J, Speck O. Point spread function mapping with parallel imaging techniques and high acceleration factors: fast, robust, and flexible method for echo-planar imaging distortion correction. *Magn Reson Med* 2004;52:1156-1166.
54. Cusack R, Brett M, Osswald K. An evaluation of the use of magnetic field maps to undistort echo-planar images. *NeuroImage* 2003;18:127-142.
55. De Martino F, Esposito F, van de Moortele PF, et al. Whole brain high-resolution functional imaging at ultra high magnetic fields: an application to the analysis of resting state networks. *NeuroImage* 2011;57:1031-1044.
56. Wiggins GC, Polimeni JR, Potthast A, et al. 96-Channel receive-only head coil for 3 Tesla: design optimization and evaluation. *Magn Reson Med* 2009;62:754-762.